Materials Science-Poland, Vol. 25, No. 1, 2007

Transport properties of as-deposited cadmium phthalocyanine Schottky-barrier devices

MAMMEN SAMUEL*, C. S. MENON, N. V. UNNIKRISHNAN

School of Pure and Applied Physics, Mahatma Gandhi University, Kottayam-686 560, Kerala, India

Sandwich samples of the type (Au–CdPc–Al) have been fabricated by successive vacuum deposition of gold (Au), cadmium phthalocyanine (CdPc), and aluminium (Al) thin films on glass substrates. Good rectification properties have been observed in the device. Ohmic conduction in the lower voltage range has been identified from the forward bias current density-voltage characteristics at room temperature. At higher voltages, a space charge limited conductivity (SCLC) controlled by an exponential trapping distribution above the valence band edge has been observed. The transport properties of the material at ambient temperature have been obtained from an analysis of the samples in the SCLC region. Schottky emission has been identified at lower voltages from the analysis of the reverse bias characteristics.

Key words: transport properties; Schottky barrier; organic semiconductor

1. Introduction

Metal phthalocyanines (MPcs) are generally p-type semiconductors and have the advantage of being sufficiently stable towards chemical and thermal treatment. They can easily be vacuum deposited, resulting in high purity thin films without decomposition. Electronic devices with MPcs as the active materials can be fabricated on a wide variety of substrates, including flexible materials. Many of them have been extensively studied in recent years due to their potential applications in thin-film electronic devices such as light emitting devices [1], transistors [2–4], photovoltaic cells [5, 6], and in photoreceptor devices such as laser beam printers and photocopiers [7]. Basic electrical conduction processes observed in these materials depend on many factors, including the phthalocyanine species, film thickness, film deposition temperature, and the electrode materials. DC electrical studies of thin-film heterostructures of the metal–organic semiconductor–metal type have provided lots of information regarding the electrical conduction mechanism, transport properties, characteristics of

*Corresponding author, e-mail: masabe@rediffmail.com

metal-organic semiconductor interfaces, etc. [8–10]. Such information is vital in the development of high performance thin film electronic devices. Among various phthalocyanines, cadmium phthalocyanine (CdPc) has received considerably less attention. The object of this paper is to investigate the transport properties of cadmium phthalocyanine (CdPc) thin films using Ohmic gold [11, 12] and blocking aluminium [13, 14] electrodes.

2. Experimental

Cadmium phthalocyanine (CdPc) powder (Aldrich Chemicals, USA) purified by train-sublimation using nitrogen gas as a carrier [14, 15] was used as the source material. Three-layer sandwich samples were prepared on glass substrates by sequential vacuum thermal evaporation in a single vacuum cycle, using a Hind Hivac 12A4 evaporation plant under the base pressure of 10^{-3} Pa. A thin layer of gold (~100 nm) was first deposited onto a pre-cleaned glass substrate from an electrically heated tungsten spiral. Over this, a CdPc layer was deposited using an electrically heated molybdenum boat. Finally, an aluminium layer with thea thickness of ~100 nm was deposited using another tungsten spiral. The thickness of the film was measured using Tolansky's multiple beam interference technique [16]. Sandwich structures with an effective area of 2.0×10^{-5} m^2 and CdPc layer thicknesses of 240 nm, 315 nm, 410 nm, and 485 nm were used in the analysis. A Keithley electrometer (model No. 617) was used for the current–voltage measurements. Temperature measurements were performed with a Chromel-Alumel thermocouple placed in close proximity of the samples. To avoid contamination and any photoelectric effects, all measurements were performed under a subsidiary vacuum of 10^{-1} Pa in a lightproof conductivity cell. Capacitance measurements were done using a Hioki 3532 LCR Hi-tester.

3. Results and discussion

The current–voltage (*I–V*) characteristics of the Au–CdPc–Al device (240 nm) are shown in Fig. 1. The forward bias direction corresponds to the positive Au (bottom) electrode and negative Al (top) electrode of the device. The characteristics as shown in Fig. 1 are attributed to the low work function of Al and high work function of Au electrodes and to the p-type conduction of CdPc. Detailed information about the transport mechanism through the organic thin film can be obtained from an analysis of the forward current density–voltage (*J–V*) characteristics of the device. The forward *J–V* characteristics are shown in Fig. 2. At low voltages, the slope of log J vs. log V is around unity (1.06), and at higher voltages, above a well-defined voltage V_x, this slope is 3.26. These slopes indicate an Ohmic region due to thermally generated carriers at lower voltages and a power-law region at higher voltages typical of a space-charge-limited conduction (SCLC) mechanism controlled by the presence of traps distributed exponentially with energy within the band gap of the CdPc.

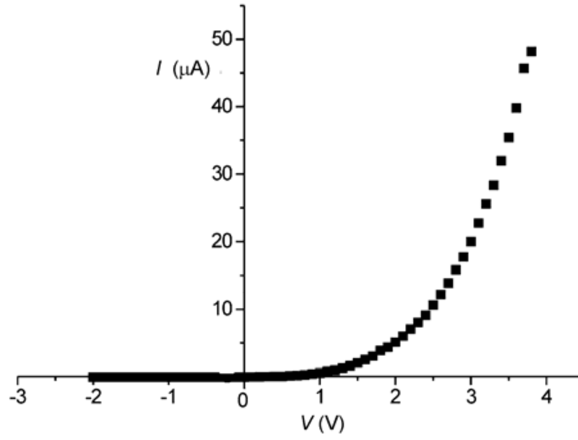

Fig. 1. Current–voltage characteristics
of the Au–CdPc–Al device at room temperature

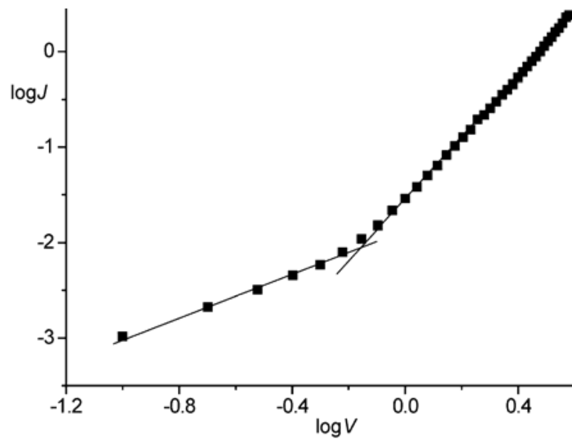

Fig. 2. Plot of log J [A·m^{-2}] vs. log V [V] at 300 K.
The lower voltage region corresponds to Ohmic conductivity
and the higher one corresponds to SCLC

Shown in Fig. 3 is the thickness dependence of forward current density J at room temperature for various applied voltages in the Ohmic region. Slopes of ~ –1 provide evidence of Ohmic conductivity at low voltages, satisfying the current density–voltage relation [17]:

$$J = ep\mu\left(\frac{V}{d}\right) \tag{1}$$

where p is the concentration of thermally generated holes in the valence band, e is the electronic charge, μ is hole mobility, V is the applied DC voltage, and d is the thickness of CdPc thin film.

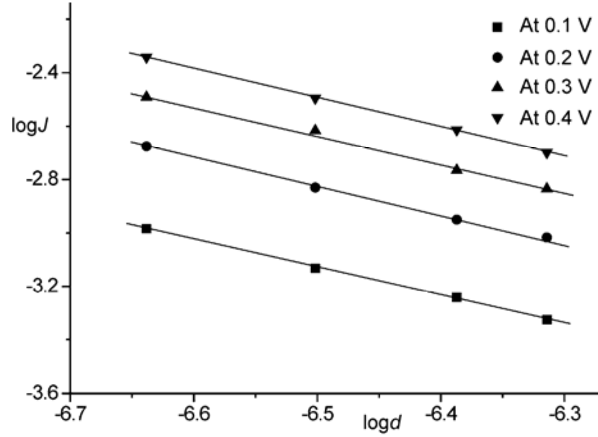

Fig. 3. Dependence of log J on thickness (log$d$) for the various applied voltages in the Ohmic region at room temperature; d is expressed in meters

Within the SCLC region, the current density J is given by [18, 19]

$$J = e\mu N_V \left(\frac{\varepsilon_r \varepsilon_0}{eP_0 k_B T_t} \right)^L \frac{V^{L+1}}{d^{2L+1}} \tag{2}$$

where P_0 is the trap density per unit energy range at the valence band edge, ε_0 is the permittivity of free space (8.85×10^{-12} F·m^{-1}), ε_r is the relative permittivity of the sample ($\varepsilon_r = 3.08$ is obtained from capacitance measurements), and L is the ratio T_t / T where T is the ambient temperature, T_t is a temperature parameter describing the exponential trapping distribution, and k_B is the Boltzmann constant. The exponential trap distribution may be described in terms of T_t as [14,19]

$$P(E) = P_0 \exp\left(\frac{-E}{k_B T_t} \right) \tag{3}$$

where $P(E)$ is trap concentration per unit energy range at an energy E above the valence band edge. In Eq. (2), the slope of 3.26 implies that $L = 2.26$ and thus the temperature parameter $T_t = 678$ K for $T = 300$ K. Figure 4 shows the thickness dependence of current density for the SCLC region at room temperature for various applied voltages. The slopes of ~ –5.6 provide evidence of SCLC conductivity satisfying Eq. (2) at higher voltages. Figure 5 shows the log J vs. $1/T$ in the SCLC region at $V = 2.0$ V for the sample with a CdPc thickness of 240 nm. For the temperature range within which samples were investigated, the characteristics show a linear fit whose slope derived from Eq. (2) is given by

$$S = T_t \log\left(\frac{\varepsilon_o \varepsilon_r V}{ed^2 P_0 k_B T_t} \right) \tag{4}$$

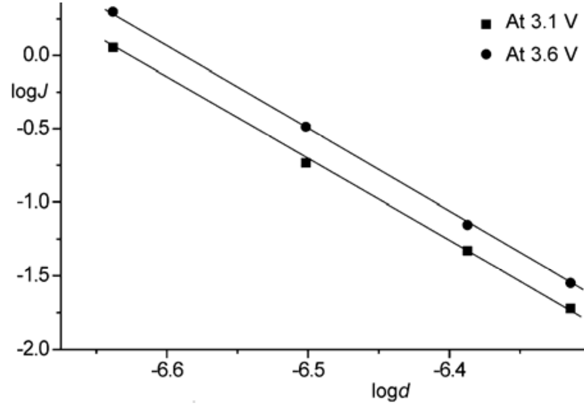

Fig. 4. Dependence of log *J* on thickness (log*d*) for the various applied voltages in the SCLC region at room temperature

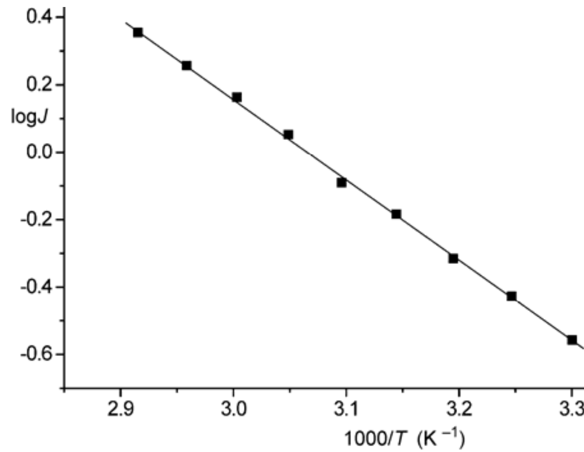

Fig. 5. Plot of log *J* versus 1000/*T* in the SCLC region

From the slope of Fig. 5, P_0 is determined equal to 2.12×10^{45} $J^{-1}\cdot m^{-3}$. The total concentration of the traps is given by [14,19]

$$N_t = P_0 k_B T_t \tag{5}$$

and is equal to 1.98×10^{25} m^{-3}. The trap concentration ranging from 10^{22} to 10^{25} m^{-3} is usually found in phthalocyanine thin films [15, 20, 21]. The intercept on the log *J* axis in Fig. 5 as obtained from Eq. (2) is given by

$$\log J_0 = \log\left(\frac{e\mu N_V V}{d}\right) \tag{6}$$

where J_0 represents the current density at infinite temperature ($1/T = 0$) and gives the value of μN_V. Taking $N_V = 10^{27}$ m^{-3}, which corresponds to one state per molecule

[13, 14, 17], the as-measured mobility μ = 1.61×10^{-8} $m^2\cdot V^{-1}\cdot s^{-1}$. Here, it is to be noted that temperature- and field-dependent mobilities are observed in several organic materials. The present work does not include an investigation on the temperature and field dependence of the mobility of the material.

The changeover from Ohmic to SCLC conduction takes place at a particular voltage V_x, known as the transition voltage. V_x is obtained from Eqs. (1) and (2) as

$$V_x = \left(\frac{p}{N_V}\right)^{1/L} \frac{ed^2 P_0 k_B T_t}{\varepsilon_0 \varepsilon_r} \tag{7}$$

At ambient temperature, $V_x \sim 0.71$ V. Using Eq. (7), the thermally generated hole concentration (p) at room temperature is 1.04×10^{18} m^{-3}.

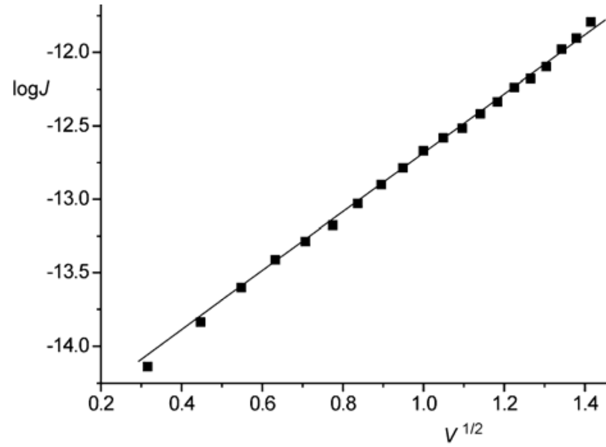

Fig. 6. Dependence of log J on $V^{1/2}$ for the reverse-biased device

The reverse bias I–V characteristics give information about the properties of the metal-semiconductor contact. Figure 6 shows the reverse bias characteristics plotted with ln$J$ against $V^{1/2}$. This linear plot can be analysed in terms of the two field-lowering mechanisms, namely, the Schottky effect and Poole–Frenkel effect. The J–V expression for the Schottky effect is given by [22, 23]:

$$J = A^* T^2 \exp\left(\frac{-\phi}{k_B T}\right) \exp\left(\frac{e\beta_S V^{1/2}}{k_B T d^{1/2}}\right) \tag{8}$$

and for the Poole–Frenkel effect it is given by

$$J = J_{PF} \exp\left(\frac{e\beta_{PF} V^{1/2}}{k_B T d^{1/2}}\right) \tag{9}$$

In these expressions, $A^* = 1.2\times10^{-6}$ A·m^{-2} is the Richardson constant, ϕ is the Schottky barrier at the injecting electrode interface, and J_{PF} is the low-field current density. β_S and β_{PF} are the Schottky and Poole-Frenkel field-lowering coefficients, respectively, related by [22]

$$2\beta_S = \beta_{PF} = \left(\frac{e}{\pi\varepsilon_0\varepsilon_r}\right)^{1/2} \tag{10}$$

This gives $\beta_S = 2.16\times10^{-5}$ eV m$^{1/2}$·V$^{-1/2}$ and $\beta_{PF} = 4.32\times10^{-5}$ eV m$^{1/2}$·V$^{-1/2}$. The value of β resulting from the slope in Fig. 6 is 2.55×10^{-5} eV m$^{1/2}$·V$^{-1/2}$. It is in reasonable agreement with the computed value of β_S, rather than the computed value of β_{PF} obtained from Eq. (10). Thus, in the case of field-lowering behaviour, the Schottky emission may be confirmed for the voltage range within which the samples were studied. The observed variance of the experimental value of β_S with respect to the theoretical value of β_S obtained from Eq. (10) is attributed to the fact that the entire thickness d of the film is not depleted. From the intercept on the ln$J$ axis in Fig. 6 and from Eq. (8), the Schottky barrier height of $\phi = 1.03$ eV was obtained. Using the theoretical value of β_S together with the slope in Fig. 6, the Schottky barrier width of ω = 172 nm was obtained. J–V characteristics typical of the Schottky barrier have also been observed in some other phthalocyanine–aluminium interface structures [18, 19, 22, 24].

4. Conclusions

I–V characteristics typical of a rectifier have been observed in the device. Under forward bias, the electrical characteristics of as-deposited devices show Ohmic conduction at low voltages. At higher voltages, space-charge limited conduction controlled by an exponential distribution of traps above the valence band edge is observed. The high concentration of traps is thought to be effective in establishing the space-charge layer. The transport parameters, derived at room temperature, are consistent with the values reported for some other MPcs. Under reverse bias, the low field conductivity is limited by the Schottky barrier 172 nm wide and 1.03 eV high.

Acknowledgement

One of the authors, M.S., is grateful to the University Grants commission of India for providing a teacher fellowship under the FIP scheme.

References

[1] FUJII A., OHMORI Y., YOSHINO K., IEEE Trans. Electron Devices, 44 (1997), 1204.
[2] JOSEPH C. M., MENON C. S., Mater. Lett., 52 (2002), 220.

[3] JOSEPH C. M., NARAYANANUNNI K. N., MENON C. S., Mater. Lett., 50 (2001), 18.
[4] JIAN Z., JUN W., HAIBO W., DONGHANG Y., Appl. Phys. Lett., 84 (2004), 142.
[5] LAW K.Y., Chem. Rev., 93 (1993), 449.
[6] RUDIONO., SHUICHI O., MANABU T., Thin Solid Films, 334 (1998), 187.
[7] BORSENBERGER P. M., WEISS D. S., *Organic Photoreceptors for Imaging Systems*, Marcel Dekker, New York, 1993.
[8] REDDY N.V., RAO B.S., RAO V.V.R.N., Mater. Lett., 13 (1992), 147.
[9] RUSU M., RUSU G.I., Appl. Surf. Sci., 126 (1998), 246.
[10] CHOPRA K.L., *Thin Film Phenomena*, McGraw-Hill, New York, 1969.
[11] GRAVANO S., HASSAN A.K., GOULD R.D., Int. J. Electron., 70 (1991), 477.
[12] GOULD R.D., Coord. Chem. Rev., 156 (1996), 237.
[13] GOLD R.D., HASSAN A.K., Thin Solid Films, 193/194 (1990), 895.
[14] RIAD A. S., Physica B, 270 (1999), 148.
[15] ABDEL-MALIK T.G., AHMED A. A., RIAD A. S., Phys. Stat. Sol. A, 121 (1990), 507.
[16] MAISSEL L.I., GLANG R., *Handbook of Thin Film Technology*, McGraw-Hill, New York, 1985.
[17] ABDEL-MALIK T.G., ABDEL-LATIF R.M., Thin Solid Films, 305 (1997), 336.
[18] MAMMEN SAMUEL, MENON C.S., UNNIKRISHNAN N.V., Semicond. Sci. Technol., 21 (2006), 677.
[19] MAMMEN SAMUEL, MENON C.S., UNNIKRISHNAN N.V., J. Phys.: Condens. Matter., 18 (2006), 135.
[20] ABDEL-MALIK T.G., Int. J. Electron., 72 (1992), 409.
[21] SHAFAI T. S., GOULD R.D., Int. J. Electron., 69 (1990), 3.
[22] SHARMA G.D., Synth. Metals, 74 (1995), 227.
[23] SZE S.M., *Physics of Semiconductor Devices*, Wiley, New York, 1969, p. 496.
[24] FAN F.R., FAULKNER L.R., J. Chem. Phys., 69 (1978), 3334.

Received 5 June 2006
Revised 14 August 2006